Growth mechanisms of highly mismatched AlSb on a Si substrate

G. Balakrishnan, S. Huang, L. R. Dawson, Y.-C. Xin, P. Conlin, and D. L. Huffaker[a)]
Center for High Technology Materials, University of New Mexico, 1313 Goddard SE, Albuquerque, New Mexico 87106

We describe the growth mechanisms of highly mismatched ($\Delta a_o/a_o = 13\%$) defect-free AlSb on Si(001) substrates. Nucleation occurs during the first few monolayers of AlSb deposition by crystalline quantum dot formation. With continued growth, the islands coalesce into a bulk material with no vertically propagating defects. Strain energy from the AlSb/Si interface is dissipated by crystallographic undulations in the zinc-blende lattice, as confirmed by high-resolution transmission electron microscopy (TEM) images. Reciprocal space analysis of the TEM images corroborates a crystallographic rotation associated with the undulations. The resulting AlSb material is >98% relaxed according to x-ray diffraction analysis. © *2005 American Institute of Physics.*
[DOI: 10.1063/1.1850611]

The growth of III-V materials on Si has been pursued for two decades to facilitate the monolithic integration of light emitters with existing Si device technology.[1–6] Research efforts in the late 1980s culminated in the demonstration of room-temperature GaAs/AlGaAs lasers[2] and even vertical cavity lasers grown on Si(100).[3] While these results were encouraging at the time, the device characteristics were only marginal due to microcracks and high dislocation density in the GaAs buffer.[4] Several growth methods were developed to improve the GaAs buffer, the two most notable of which are a low As/Ga ratio and *in situ* thermal cycling.[5] More recently, off-axis substrates and low-temperature growth techniques were invoked to nucleate GaAs growth on Si for InGaAs quantum dot (QD)-based lasers.[6] However, the GaAs buffer was dominated by dark-line defects that originate at the GaAs/Si interface.[7]

In comparison with GaAs and other III-V materials, AlSb has been shown to produce defect-free buffers on lattice mismatched substrates.[8] In previously published work, growth of AlSb on GaAs ($\Delta a_o/a_o = 7.8\%$) results in optically smooth surfaces as viewed by Nomarski microscopy and very few threading dislocations according to transmission electron microscopy (TEM) analysis. The growth of AlSb on Si was first explored in the mid-1980s by Van der Ziel and co-workers. This work led to double-heterostructure lasers ($J_{th} = 13$ kA/cm^2) and photodetectors.[9] However, the growth mechanisms of the highly lattice mismatched epitaxy have not been identified.

In this letter, we explain both the nucleation and the strain-relief mechanisms in high quality AlSb growth on Si. First, we show that the nucleation layer is comprised of a crystalline AlSb QD ensemble. With continued deposition, the islands coalesce into a bulk material in which the strain energy from the AlSb/Si interface is dissipated by crystallographic undulations. Crystallographic undulations provide additional surface area to accommodate strain and have been noted as a strain-relief mechanism in the compliant substrate technology.[10–12]

Prior to growth, the Si substrate surface is hydrogen passivated in an HF etch. The hydrogen is removed by heating the substrate to 500 °C in vacuum. A thermal cycle at 800 °C ensures that any remnants of the oxide are removed. The removal of the hydrogen is verified by reflection high-energy electron diffraction (RHEED). The substrate temperature is reduced and stabilized at 500 °C followed by a 5 min soak in an Sb overpressure.

Figures 1(a)–1(c) show atomic force microscopy (AFM) data after 3, 18, and 54 monolayers (ML) of AlSb deposition, respectively. At 3 ML, the QD density is 10^{11} QD/cm^2 with dot height and diameter of 1–3 nm and 20 nm, respectively.[14] Figure 1(b) shows the growth at 18 ML. The effect of this continued deposition causes the individual islands to coalesce, but they remain crystallographic, in contrast to InAs/GaAs QD growth, in which island coalescence leads to large defective islands.[13,14] Figure 1(c) shows continued coalescence towards planar growth with 54 ML deposition. The insets show corresponding RHEED patterns at each stage of the nucleation layer growth. At 3 ML, the RHEED pattern is spotty with overlaid chevrons characteristic of QD growth. After 54 ML deposition, the spotty/chevron character has transformed to a streaky 3×1 pattern associated with planar growth after 54 ML deposition.

Figure 2 shows a cross-sectional high-resolution TEM (HR-TEM) image of the (110) crystal plane at the AlSb/Si interface. The image shows three distinct regions labeled (i), (ii), and (iii), respectively. Region (i) is the white line along the interface that is an artifact of the initial AlSb nucleation on Si. The deteriorated resolution in this region compared to the surrounding material makes analysis of this region is difficult. The white appearance in contrast to the surrounding material indicates a higher density of atoms compared to the
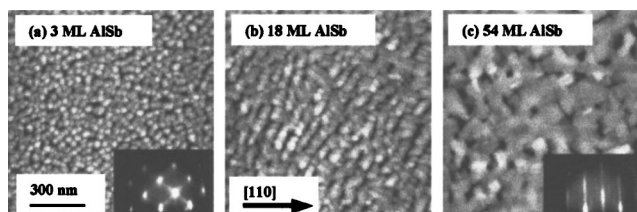

FIG. 1. AFM images showing surface structure after (a) 3 ML, (b) 18 ML, and (c) 54 ML of AlSb deposition on Si. (a) and (c) RHEED images for the corresponding growths.
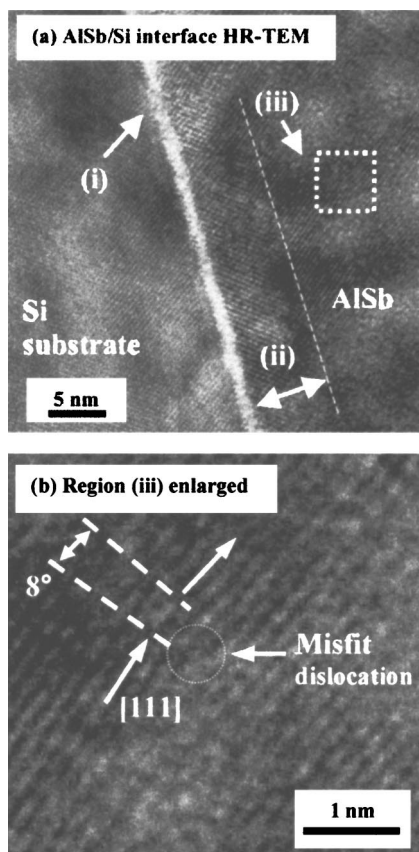
[a)]Electronic mail: huffaker@chtm.unm.edu

FIG. 2. Cross-sectional HR-TEM image of the AlSb/Si interface, showing the (110) plane. (b) Magnified section of part (a), showing a change in crystallographic orientation and a misfit dislocation that results from it.
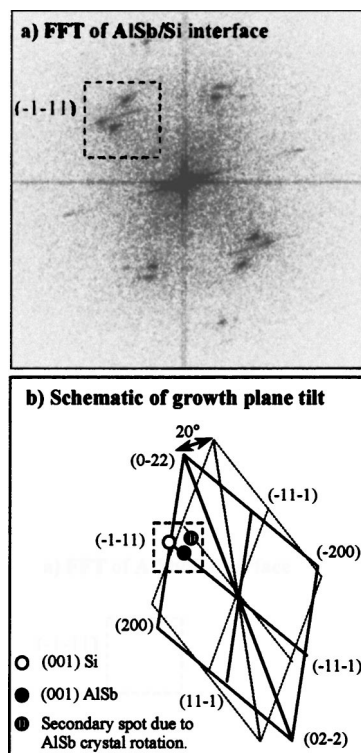

FIG. 3. Fast Fourier transform of a HR-TEM image of AlSb/Si interface. (b) Schematic of (a), showing the presence of an additional AlSb lattice rotated by 20° clockwise to the (100) plane. The $(-1-11)$ component has been used to illustrate the effect.

surrounding (110) plane, possibly due to a twisted lattice. Artificially induced twist-bonded substrates have been known to accommodate considerable interfacial mismatch and lead to undulations, as described by Ejeckam *et al.*[10–12] Region (ii), about 5 ML in thickness, represents the nucleation layer formed by QD growth and coalescence. This material is defect free and shows a planar, homogeneous zincblende crystal structure in which the arrangement of the atoms is in the form of consecutive (100) planes. In contrast, region (iii) contains undulating bulk material, denoted by a measurable rotation of the zinc-blende crystal lattice. Region (iii) is magnified in Fig. 2(b) to elucidate the clockwise rotation of the lattice (8°) with respect to the [111] direction. The crystallographic undulations or bending lead to misfit dislocations that propagate parallel to the substrate. One such misfit dislocation is visible in Fig. 2(b) and has been labeled. In other material systems, such as growth of InAs on GaAs, misfit dislocations lead to vertical propagating defects, such as threading or screw dislocations. However, the AlSb does not propagate these vertical defects due to the strong Al–Sb bond at these growth temperatures.

Figure 3 shows the reciprocal space analysis of Fig. 2(a) that includes regions (i), (ii), and (iii). The schematic illustrates the components associated with the reciprocal view of a [110] plane within the zinc-blende and diamond lattice. In analyzing the $(-1-11)$ component, three spots are indicated. One spot indicates the Si(100) lattice. A second spot, located closer to the (000) point, corresponds to the AlSb(100). A third spot corresponds to the AlSb point on a rhombus rotated clockwise by 20°. This indicates a completely different

plane of growth from the (100) plane. A range of crystallographic rotations, both clockwise and counter-clockwise, are measured at other locations within this sample. The crystallographic rotations measured in the reciprocal image are indicative of undulations in the AlSb bulk and corroborate the real-space TEM analysis of Fig. 2.

Figure 4 shows TEM images of the undulations at the AlSb surface after 70 ML of AlSb growth on Si. The figure also shows a layer of native oxide on the sample surface that forms quickly during atmospheric exposure. The surface undulations are $\sim$10 nm wide and 1 nm high. We estimate the misfit dislocation density to be $\sim$10^{10}/cm^2 at this point in the growth process. With continued growth ($\sim$1 μm), the surface undulations merge, become shallower and considerably broader until they can no longer be detected by TEM. However, evidence of the undulation is still visible in the RHEED pattern for very thick ($\sim$10 μm) AlSb layers. Misfit
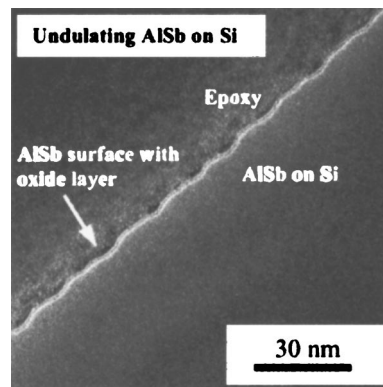

FIG. 4. Cross-sectional TEM of AlSb on Si, showing the undulating surface.

dislocation density should also decrease significantly as the undulations become shallow and broad. Analysis by high-resolution x-ray diffraction (data not shown) using a combination of (004) and (115) scans of an AlSb layer (500 nm) grown on Si indicates the relaxation of the AlSb to be ~98%. As a general indication of AlSb buffer material quality, we have demonstrated room-temperature photoluminescence at 1.7 μm from $In_{0.10}Ga_{0.90}Sb$ quantum wells grown on AlSb/Si.

In conclusion, we have identified the growth mechanisms of highly mismatched AlSb on Si. The initial nucleation occurs by self-assembled QDs. The continuation of growth leads to QD coalescence followed by undulations in the AlSb. The undulations increase the surface area of the AlSb and provide strain relief. The undulating material contains misfit dislocations parallel to the (100) plane; however, these do not propagate vertically as threading or screw dislocations. The AlSb layers provide a template for future III-V devices on Si.

[1] T. H. Windhorn, G. M. Metze, B. Y. Tsaur, and J. C. Fan, Appl. Phys. Lett. **45**, 309 (1984).

[2] D. G. Deppe, N. Holonyak, Jr., D. W. Nam, K. C. Hsieh, G. S. Jackson, R. J. Matyi, H. Shichiujo, J. E. Epler, and H. F. Chung, Appl. Phys. Lett. **51**, 637 (1987).

[3] D. G. Deppe, Naresh Chand, J. P. van der Ziel, and G. J. Zydzik, Appl. Phys. Lett. **56**, 740 (1990).

[4] D. G. Deppe, N. Holonyak, Jr., K. C. Hsieh, D. W. Nam, And W. E. Plano, R. J. Matyi, and H. Shichijo, Appl. Phys. Lett. **52**, 1812 (1988).

[5] Naresh Chand, F. Ren, A. T. Macrander, J. P. van der Ziel, A. M. Sergent, R. Hull, S. N. G. Chu, Y. K. Chen, and D. V. Lang, J. Appl. Phys. **67**, 2343 (1990).

[6] K. K. Linder, J. Phillips, O. Qasaimeh, X. F. Liu, S. Krishna, P. Bhattacharya, and J. C. Jiang, Appl. Phys. Lett. **74**, 1355 (1999).

[7] R. Heitz, N. N. Ledentsov, D. Bimberg, A. Yu. Egorov, M. V. Maximov, V. M. Ustinov, A. E. Zhukov, Zh. I. Alfereove, G. E. Cirlin, I. P. Soshnikov, N. D. Zakharov, P. Werner, and U. Gosele, Appl. Phys. Lett. **74**, 1701 (1999).

[8] Chin-An Chang, H. Takaoka, L. L. Chang, and L. Esaki, Appl. Phys. Lett. **40**, 983 (1982).

[9] J. P. van der Ziel, R. J. Malik, J. F. Walker, and R. M. Mikulyak, Appl. Phys. Lett. **48**, 454 (1986).

[10] F. E. Ejeckam, M. L. Seaford, Y.-H. Lo, H. Q. Hou, and B. E. Hammons, Appl. Phys. Lett. **71**, 776 (1997).

[11] M. L. Seaford, P. J. Hesse, D. H. Tomich, and K. G. Eyink, J. Electron. Mater. **28**, 878 (1999).

[12] F. E. Ejeckam, C. L. Chua, Z. H. Zhu, Y. H. Lo, M. Hong, and R. Bhat, Appl. Phys. Lett. **67**, 3936 (1995).

[13] G. Balakrishnan, S. Huang, L. R. Dawson, Y.-C. Xin, P. Conlin, and D. L. Huffaker (unpublished).

[14] Z. L. Liau and D. E. Mull, Appl. Phys. Lett. **56**, 737 (1990).